

Creating Poly(ethylene oxide)-Based Polyelectrolytes for Thin Film Construction Using an Ionic Linker Strategy

Yao Wang, Vaclav Janout, and Steven L. Regen*

Department of Chemistry, Lehigh University,
Bethlehem, Pennsylvania 18015

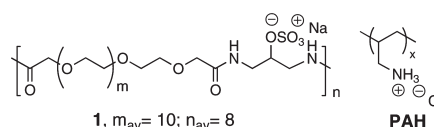
Received November 23, 2009

Revised Manuscript Received January 15, 2010

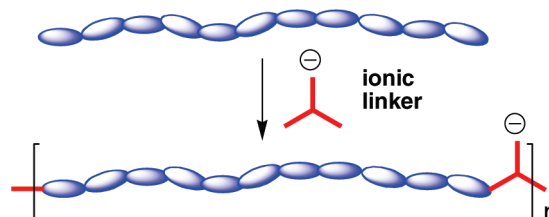
In this paper, we show that poly(ethylene oxide) (PEO) can be converted into a polyelectrolyte using an ionic linker, and that this polymer is suitable for forming polyelectrolyte multilayers (PEMs). Specifically, we show that **1** can combine with poly(allylamine hydrochloride) (PAH) to form (PEMs) via layer-by-layer (LbL) deposition methods (Chart 1). We also show that such materials exhibit reverse size-selectivity in which the permeation of a relatively large CO₂ molecule is favored over He, and that their permeation selectivity with respect to CO₂/N₂ is exceptional. The potential of this new synthetic approach for modifying the bulk properties of PEMs is briefly discussed.

Polymers that contain poly(ethylene oxide) (PEO) are of considerable current interest as membrane materials for the separation of acid gases from light gases and hydrocarbons, e.g., the removal CO₂ from H₂/CO₂ and CO₂/N₂.^{1–8} The main virtue of PEO for such separations is its affinity toward CO₂, which results in relatively high solubility and permeability.¹ In principle, the creation of ultrathin PEO-based films that combine high flux rates with such selectivity properties could lead the way to

Chart 1



Scheme 1



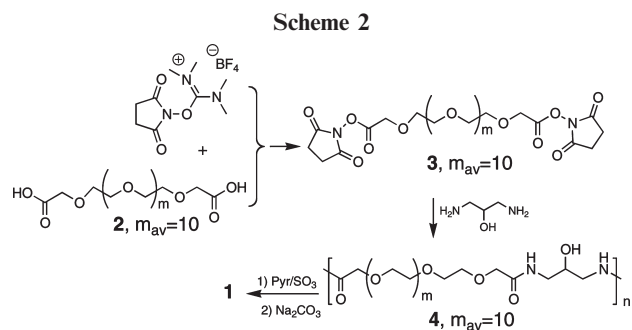
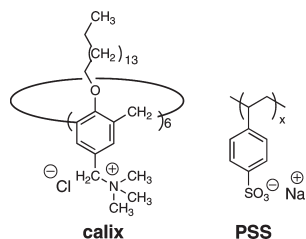
advanced materials and processes for the purification of hydrogen, as well as the removal of CO₂ from flue gases. While there have been several reports in the literature of gas permeation across PEMs, to the best of our knowledge, none have demonstrated the feasibility of reverse size-selectivity with film thicknesses below 10 nm.⁹

Although PEO can be combined with carboxylic acid-containing polymers to form thin films via the LbL method, the use of hydrogen bonds to hold such assemblies together makes them susceptible to weakening and disassembly by permeants that can compete for hydrogen bonding, e.g., acid gases.^{10–14} In principle, analogous films that are based on ionic bonds should be more robust. With this idea in mind, we sought PEMs that are rich in ethylene oxide content. While certain PEO-based diblock copolymers have been used to prepare polyelectrolyte complexes and polyelectrolyte multilayers (PEMs), we sought a fundamentally new structural motif that would allow us to maximize the PEO content and minimize the number of pendant ions used for self-assembly.¹⁵ The specific strategy that we explored is illustrated in Scheme 1, whereby an ionic linker is used to join a series of PEOs. Our working hypothesis was that a relatively a low concentration of well-spaced, pendant ions would be sufficient to allow for PEM formation and that the resulting thin film would exhibit reverse size-selectivity.

*Corresponding author. E-mail: slr0@lehigh.edu.

- (1) (a) Kusuma, V. A.; Freeman, B. D.; Borns, M. A.; Kalika, D. J. *Membr. Sci.* **2009**, 327, 195–207. (b) Lin, H.; Van Wagner, E.; Freeman, B. D.; Toy, L. G.; Gupta, R. P. *Science* **2006**, 311, 639–642. (c) Raharjo, R. D.; Lin, H.; Sanders, D. F.; Freeman, B. D.; Kalakkunnath, S.; Kalika, D. J. *Membr. Sci.* **2006**, 283, 253–265. (d) Lin, H.; Freeman, B. D. *Macromolecules* **2006**, 39, 3568–3580.
- (2) (a) Car, A.; Stroopnik, C.; Wilfredo, Y.; Peinemann, K. V. *Sep. Purif. Technol.* **2008**, 62, 110–117. (b) Car, A.; Stroopnik, C.; Wilfredo, Y.; Peinemann, K. V. *J. Membr. Sci.* **2008**, 307, 88–95.
- (3) Zhao, H.-Y.; Cao, Y.-M.; Ding, X.-L.; Zhou, M.-Q.; Yuan, Q. *J. Membr. Sci.* **2008**, 310, 365–373.
- (4) Bai, H.; Ho, W. S. W. *Ind. Eng. Chem. Res.* **2009**, 48, 2344–2354.
- (5) Ockwig, N. W.; Nenoff, T. M. *Chem. Rev.* **2007**, 107, 4078–4110.
- (6) Taniguchi, I.; Duan, S.; Kazama, S.; Fujioka, Y. *J. Membr. Sci.* **2008**, 322, 277–280.
- (7) Charmette, C.; Sanchez, J.; Gramain, P.; Masquelez, N. *J. Membr. Sci.* **2009**, 344, 275–280.
- (8) Powell, C. E.; Qiao, G. G. *J. Membr. Sci.* **2006**, 279, 1–49.
- (9) (a) Tieke, B. In *Handbook of Polyelectrolytes and Their Applications*; Nalwa, H. S., Ed.; American Scientific: Valencia, CA, 2002; Vol. 3, pp 115–124. (b) Tieke, B.; El-Hashani, A.; Toutianoush, A.; Fendt, A. *Thin Solid Films* **2008**, 516, 8814–8820. (c) Sullivan, D. M.; Bruening, M. L. *Chem. Mater.* **2003**, 15, 281–287. (d) Bruening, M. L.; Dotzauer, D. M.; Jain, P.; Ouyang, L.; Baker, G. L. *Langmuir* **2008**, 24, 7663–7673. (e) Leväsalmi, J. M.; McCarthy, T. J. *Macromolecules* **1995**, 28, 1733–1738. (f) Leväsalmi, J. M.; McCarthy, T. J. *Macromolecules* **1997**, 30, 1752–1757.

- (10) Stockton, W. B.; Rubner, M. F. *Macromolecules* **1997**, 30, 2717–2725.
- (11) (a) Sukhishvili, S. A.; Granick, S. *J. Am. Chem. Soc.* **2000**, 122, 9550–9551. (b) Sukhishvili, S. A.; Granick, S. *Macromolecules* **2002**, 35, 301–310.
- (12) Quinn, J. F.; Caruso, F. *Macromolecules* **2005**, 38, 3414–3419.
- (13) (a) Seo, J.; Lutkenhaus, J. L.; Kim, J.; Hammond, P. T.; Char, K. *Langmuir* **2008**, 24, 7995–8000. (b) Lutkenhaus, J. L.; Krabak, K. D.; McEnnis, K.; Hammond, P. T. *J. Am. Chem. Soc.* **2005**, 127, 17228–17234. (c) DeLongchamp, D. M.; Hammond, P. T. *Langmuir* **2004**, 20, 5403–5411.
- (14) Kharlampieva, E.; Sukhishvili, S. A. *J. Macromol. Sci., Part C: Polym. Rev.* **2006**, 46, 377–395.
- (15) Salloum, D. D.; Loenych, S. G.; Keller, T. C. S.; Schlenoff, J. B. *Biomacromolecules* **2005**, 6, 161–167.

**Chart 2**

To test our hypothesis, we synthesized **1** using a reaction sequence that is outlined in Scheme 2. Thus, activation of **2** (Aldrich) with *N,N,N',N'*-tetramethyl-*O*-(*N*-succinimidyl)uronium tetrafluoroborate (TSTU) to give the corresponding diester, **3**, followed by condensation with 1,3-diamino-2-propanol afforded **4**. Subsequent persulfation with pyridine/ SO_3 and ion exchange with Na_2CO_3 yielded **1**.

To test for PEM formation, we modified the surface of a silicon wafer by silylation with *n*-octadecyltrichlorosilane (OTS), followed by deposition of a Langmuir–Blodgett monolayer of 5,11,17,23,29,35-hexakis[*N,N,N*-trimethylammonium)-*N*-methyl-37,38,39,40,41,42-hexakis-*n*-hexadecyloxy-calix[6]arene hexachloride (i.e., “calix”) that was ionically cross-linked with poly(4-styrene sulfonate) (i.e., PSS) (Chart 2).¹⁶ For convenience, we refer to the latter as calix-PSS. Subsequent alternate dipping into aqueous solutions of PAH and **1** with intermediate washings gave ellipsometric film thicknesses that increased with increasing numbers of layers (Figure 1). Although we do not presently understand the basis for the change in slope that is apparent after 16 layers, it should be noted that such a feature has been commonly observed with LbL films.¹⁷ Control experiments that were carried out with unfunctionalized PEO and **4** showed no such ability to form multilayers with PAH under similar conditions.

Examination of a PEM made from 13 alternate dipings of PAH and **1** by atomic force microscopy (AFM) [i.e., $(\text{PAH-1})_{13}$] showed a smooth surface with a roughness factor of 0.65 nm (Figure 2). Profilometry by AFM (after scratching the surface with a razor blade to remove

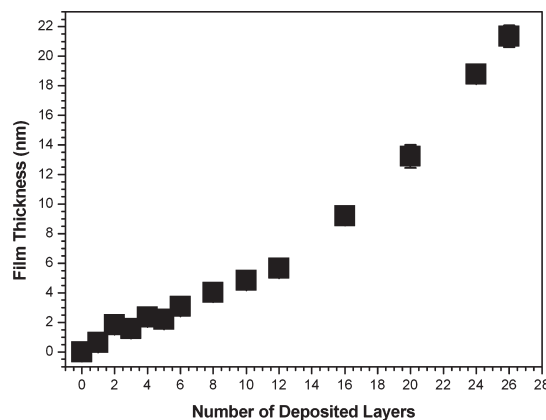


Figure 1. Plot of ellipsometric film thickness versus the number of alternating monolayers of **1** and PAH, deposited onto an OTS-silylated silicon wafer that was modified with one LB layer of calix-PSS. In all cases, the thickness of the OTS/calix-PSS layer has been subtracted from the total thickness. The error bars for each measurement lie within the symbols themselves.

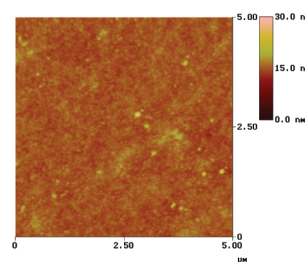


Figure 2. Height image (AFM, tapping mode, $5 \times 5 \mu\text{m}^2$) of a PEM of $(\text{PAH-1})_{13}$ that was deposited onto an OTS-modified silicon wafer bearing a single ionically cross-linked Langmuir–Blodgett monolayer of calix-PSS. The LB transfer was made using a speed of 2 mm/min and a surface pressure of 30 dyn/cm.

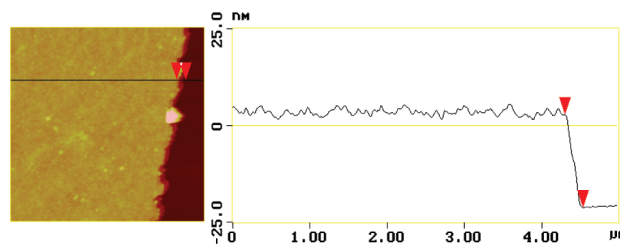


Figure 3. Height image and section profile (AFM, tapping mode, $5 \times 5 \mu\text{m}^2$) showing the film thickness of $(\text{PAH-1})_{13}$; the z-scale is shown to the right.

the film, and determining step heights) gave a film thickness for calix/PSS/ $(\text{PAH-1})_{13}$ of 23.5 ± 0.4 nm, which was in excellent agreement with an ellipsometry value of 23.5 ± 0.7 nm (Figure 3).

To determine the barrier properties of PEMs made from **1** and PAH, we deposited a series of films onto supports made from poly[1-(trimethylsilyl)-1-propyne] (PTMSP) that were coated with one LB monolayer of (calix-PSS).¹⁶ Experimental procedures that were used in carrying out alternate dipping with intermediate wash-cycles were similar to those used for the silicon substrates. The gaseous permeants used to define the barrier properties of these PEMs were He, CO_2 , and N_2 , which have

- (16) Wang, Y.; Stedronsky, E.; Regen, S. L. *J. Am. Chem. Soc.* **2008**, *130*, 16510–16511.
 (17) (a) Dubas, S. T.; Schlenoff, J. B. *Macromolecules* **1999**, *32*, 8153–8160. (b) Hübsch, E.; Ball, V.; Senger, B.; Decher, G.; Voegel, J. C.; Schaaf, P. *Langmuir* **2004**, *20*, 1980–1985. (c) Garza, J. M.; Schaaf, P.; Müller, S.; Ball, V.; Stoltz, J. F.; Voegel, J. C.; Lavalle, P. *Langmuir* **2004**, *20*, 7298–7302. (d) Ji, J.; Fu, J. H.; Shen, J. C. *Adv. Mater.* **2006**, *18*, 1441–1444.

Table 1. Permeances of Gases Across Polymer Membranes^a

membrane ^b	PEM (nm)	He	N ₂	CO ₂	He/N ₂	He/CO ₂
S		223	244	1343	0.91	0.17
S/A		227	252	1380	0.90	0.16
S/A/B ₇	7	23.7	<0.1	28.6	>237	0.83
S/A/B ₇ ^c		13.1	<0.1	17.5	>131	0.75
S/A/C ₄ /D	7	34.4	1.59	28.6	21.6	1.20
S/A/B ₁₃	21	9.17	<0.1	18.3	>92	0.50
S/A/B ₁₃ ^c		8.15	<0.1	18.1	>85	0.47
S/A/C ₇	23	26.5	<0.1	16	>265	1.66
S/A/B ₂₅	60	2.24	<0.1	6.53	>22.4	0.34

^a Permeances at ambient temperature, 1×10^6 P/l ($\text{cm}^3/(\text{cm}^2\text{-s-cm Hg})$), were calculated by dividing the observed flow rate by the area of the membrane (9.36 cm^2) and the pressure gradient (10 psi) employed, using ca. $30 \mu\text{m}$ thick PTMSP supports (S). All measurements were made at ambient temperatures. Values were obtained from 5–10 independent measurements; the error in each case was $\pm 5\%$. ^b A = (calix-PSS); B = (PAH-1); C = (PAH-PSS); D = PAH. ^c A duplicate membrane prepared from a separate batch of 1.

kinetic diameters of 0.260, 0.330, and 0.363 nm, respectively.¹⁸ Thus, based on diffusivity alone, permeation rates are expected to decrease with increasing size, i.e., $\text{He} > \text{CO}_2 > \text{N}_2$. Our use of He as a surrogate for H₂ (0.289 nm diameter) was based primarily on safety reasons because of the combustible nature of H₂ and the fact that He and H₂ behave almost the same in most gas separation experiments.

In the absence of a PEM, the bare substrate (PTMSP, S), and also a substrate containing one LB layer of (calix-PSS), showed negligible He/N₂ selectivity but significant He/CO₂ reverse-size selectivity (Table 1). When 14-monolayers of alternating PAH and 1 [i.e., (PAH-1)₇] were deposited onto the calix-PSS layer, the flux values for He, N₂ and CO₂ were substantially reduced, and the He/N₂ and He/CO₂ permeation selectivities were >237 and 0.83, respectively. In contrast, an analogous PEM of (PAH-PSS)₄PAH, which was of similar thickness, exhibited higher flux values, a significantly lower He/N₂ permeation selectivity, and barrier properties that were dominated by diffusion, as evidenced by normal size-selectivity; that is, the permeance for the larger CO₂ molecule was less than that for He.¹⁷ Increasing the thickness of such poly(ethylene oxide)-containing PEMs [i.e., (PAH-1)₁₃] resulted in a further reduction in the flux values for He and CO₂, and a net increase in reverse

size-selectivity (i.e., $\text{He}/\text{CO}_2 = 0.50$). In contrast, a PEM of (PAH-PSS)₇ that matched the thickness of (PAH-1)₁₃ showed a further increase in normal size-selectivity favoring the transport of He. Finally, a PEM that was fabricated from (PAH-1)₂₅ showed a further reduction in flux values for He and CO₂ with a corresponding increase in reverse size-selectivity, having $\text{He}/\text{CO}_2 = 0.34$. Taken together, these results indicate that (i) PEMs that are fabricated using alternating layers of PAH and 1 have greater barrier properties than those made from PAH and PSS, when films of similar thickness are compared, and (ii) a PEO-based polyelectrolyte introduces reverse size-selectivity to a PEM.

The reverse size-selectivities for these poly(ethylene oxide)-based PEMs for He/CO₂ are modest. It is noteworthy, however, that their permeation selectivity for CO₂/N₂ is exceptional; that is, ≥ 286 for a 7 nm-thick membrane.⁸ The latter may be the consequence of the enhanced solubility of CO₂ plus greater diffusivity because of its small kinetic diameter relative to N₂. It should also be noted, however, that the CO₂/N₂ selectivity for the 23 nm thick film formed from PAH/PSS (>160) is also impressive. Because of our inability to detect a flow of N₂ under the conditions used, the question of which of these two types of membranes has a higher CO₂/N₂ selectivity remains to be determined.

We believe that further improvements should be possible by combining 1 with a variety of other cationic polymers, including ones that also contain poly(ethylene oxide) segments. Studies along these lines, including stability measurements, are currently in progress. In a broader context, the ability to modify the barrier properties of a PEM using this ionic linker strategy suggests that similar approaches may allow one to modulate the bulk properties of PEMs in ways that have not previously been possible.

Acknowledgment. This work was supported by the Department of Energy (Grant DE-FG02-05ER15720). We are grateful to our colleague, Dr. Wen-Hua Chen, for valuable discussions.

Supporting Information Available: Materials and Methods used (PDF). This material is available free of charge via the Internet at <http://pubs.acs.org>.

(18) Cui, Y.; Kita, H.; Okamoto, K. *Chem. Commun.* **2003**, 2154–2155.